THE LANCET
Infectious Diseases

Supplementary appendix

This appendix formed part of the original submission. We post it as supplied by the authors.

Supplement to: Uriu K, Ito J, Zahradnik J, et al. Enhanced transmissibility, infectivity, and immune resistance of the SARS-CoV-2 omicron XBB.1.5 variant. *Lancet Infect Dis* 2023; published online Jan 31. https://doi.org/10.1016/S1473-3099(23)00051-8.

Appendix

Table of Contents

Materials and Methods

Ethics statement

All protocols involving specimens from human subjects recruited at Interpark Kuramochi Clinic was reviewed and approved by the Institutional Review Board of Interpark Kuramochi Clinic (approval ID: G2021-004). All human subjects provided written informed consent. All protocols for the use of human specimens were reviewed and approved by the Institutional Review Boards of The Institute of Medical Science, The University of Tokyo (approval IDs: 2021-1-0416 and 2021-18-0617).

Human serum collection

Convalescent sera were collected from fully vaccinated individuals who had been infected with BA.2 (9 2-dose vaccinated and 4 3-dose vaccinated; time interval between the last vaccination and infection, 4–299 days; 11–61 days after testing. n=13 in total; average age: 45 years, range: 24–82 years, 62% male) (**Figure S1E**), and fully vaccinated individuals who had been infected with BA.5 (2 2-dose vaccinated, 17 3-dose vaccinated and 1 4-dose vaccinated; time interval between the last vaccination and infection, 66–310 days; 10–23 days after testing. n=20 in total; average age: 51 years, range: 25–73 years, 45% male) (**Figure S1E**). The SARS-CoV-2 variants were identified as previously described.[1-3] Sera were inactivated at 56°C for 30 minutes and stored at –80°C until use. The details of the convalescent sera are summarized in **Table S1**.

Epidemics dynamics analysis

We modeled the epidemic dynamics of viral lineages in the USA based on the viral genomic surveillance data deposited in the GISAID database (https://www.gisaid.org/; downloaded on January 9th, 2023). In the present study, we analyzed the data from September 1, 2022. We excluded the sequence records with the following features: i) a lack of collection date information; ii) sampling in animals other than humans; iii) sampling by quarantine; iv) without the PANGO lineage information; and v) having >2% undetermined (N) nucleotide sequences. Sublineages of BQ.1.1 are summarized as BQ.1.1, and other BQ.1 sublineages are summarized as BQ.1. In addition, according to the presence or absence of S:Y144del, we classified XBB.1.5 into two groups, XBB.1.5 and XBB.1.5+ins144Y (XBB.1.5 without S:Y144del). We removed XBB from the analysis since we found that various XBB sublineages are contaminated into this category. In the downstream analysis, we only used sequences for PANGO lineages with >500 sequences in the dataset. We counted the daily frequency of each viral lineage. Subsequently, epidemic dynamics and relative R_e value for each viral lineage were estimated according to the Bayesian multinomial logistic model, described in our previous study.[2] Briefly, we estimated the logistic slope parameter β_l for each viral lineage using the model and then calculated relative R_e for each lineage r_l as $r_l = exp(\gamma\beta_l)$ where γ is the average viral generation time (2.1 days)

(http://sonorouschocolate.com/covid19/index.php?title=Estimating_Generation_Time_Of_Omicron). For parameter estimation, the intercept and slope parameters of XBB.1 were fixed at 0. Consequently, the relative R_e of XBB.1 was fixed at 1, and those of the other lineages were estimated relative to that of XBB.1. Parameter estimation was performed via the MCMC approach implemented in CmdStan v2.31.0 (https://mc-stan.org) with CmdStanr v0.5.3 (https://mc-stan.org/cmdstanr/). Four independent MCMC chains were run with 1,000 and 4,000 steps in the warmup and sampling iterations, respectively. We confirmed that all estimated parameters showed <1.01 R-hat convergence diagnostic values and >200 effective sampling size values, indicating that the MCMC runs were successfully convergent. Information on the estimated parameters is summarized in **Table S2**.

Plasmid construction

Plasmids expressing the SARS-CoV-2 spike proteins of the parental D614G (B.1.1), Omicron BA.2, BA.5, BQ.1.1 and XBB.1 were prepared in our previous studies.[1,2,4-8] Plasmids expressing the spike protein of XBB.1.5 and its derivative were generated by site-directed overlap extension PCR using pC-SARS2-S XBB.1[8] as the template and the primers listed in **Table S3**. The resulting PCR fragment was subcloned into the KpnI-NotI site of the pCAGGS vector[9] using In-Fusion® HD Cloning Kit (Takara, Cat# Z9650N). Nucleotide sequences were determined by DNA sequencing services (Eurofins), and the sequence data were analyzed by Sequencher v5.1 software (Gene Codes Corporation).

Yeast surface display

Yeast surface display binding analyses for the spike receptor-binding domains of BA.2, XBB and XBB.1.5 (residues 333–527) were performed as previously described.[1-4,7,8,10-12] Cerevisiae EBY100 yeasts and pJYDC1 plasmids with RBD genes cloned between the NdeI and BamHI sites (Addgene, Cat# 162458) as previously described.[10,11] Transformed yeasts were grown in SDCAA media (220 rpm, 30°C) and expressed overnight in expression media supplemented with bilirubin (10 nM DMSO solubilized, Sigma-Aldrich, Cat# 14370) after inoculation to OD600 0.7–1.0 (220 rpm, 20°C).[10,11] Aliquots of expressed yeast cells (100 µl) were washed in ice-cold PBSB buffer (PBS with 1 mg/ml BSA) and incubated in a series of CF®640R succinimidyl ester labeled (Biotium, Cat# 92108) ACE2 peptidase domain (residues 18–740) concentrations, PBSB buffer and 1 nM bilirubin for 8 to 12 hours. After incubation, the unbound fraction was washed by ice-cold PBSB buffer and yeasts were transferred into a 96-well plate (Thermo Fisher Scientific, Cat# 268200) and 30,000 events in gated population were automatically acquired by a CytoFLEX S Flow Cytometer (Beckman Coulter, USA, Cat#. N0-V4-B2-Y4) with FITC channel data for eUnaG2 fluorescence (Abs/Em maxima 498/527 nm) and APC channel for CF640 fluorescence (Abs/Em maxima 642/662 nm) setting. Gating, analysis and fitting with nonlinear least-squares regression using Python v3.7 protocols were described previously.[1-4,7,8,10-12]

Cell culture

HEK293T cells (a human embryonic kidney cell line; ATCC CRL-3216) and HOS-ACE2/TMPRSS2 cells (kindly provided by Dr. Kenzo Tokunaga),[13,14] a derivative of HOS cells (a human osteosarcoma cell line; ATCC CRL-1543) stably expressing human ACE2 and TMPRSS2, were maintained in Dulbecco's modified Eagle's medium (DMEM) (high glucose) (Wako, Cat# 044-29765) containing 10% fetal bovine serum (FBS) (Sigma-Aldrich Cat# 172012-500ML), 100 units penicillin and 100 ug/ml streptomycin (PS) (Sigma-Aldrich, Cat# P4333-100ML).

Pseudovirus infection

Pseudoviruses were prepared as previously described.[1-3,5-8,12,13,15-18] Briefly, lentivirus (HIV-1)-based, luciferase-expressing reporter viruses were pseudotyped with the SARS-CoV-2 spikes. HEK293T cells (1×10^6 cells) were cotransfected with 1 μg psPAX2-IN/HiBiT,[19] 1 μg pWPI-Luc2,[19] and 500 ng plasmids expressing parental S or its derivatives using PEI Max (Polysciences, Cat# 24765-1) according to the manufacturer's protocol. Two days post transfection, the culture supernatants were harvested and centrifuged. The amount of pseudoviruses prepared was quantified by the HiBiT assay using Nano Glo HiBiT lytic detection system (Promega,Cat# N3040) as previously described.[1-3,5-8,12,13,15-18] To measure viral infectivity, the same amount of pseudoviruses (normalized to the HiBiT value, which indicates the amount of p24 HIV-1 antigen) was inoculated into HOS-ACE2/TMPRSS2 cells. Two days post infection, the infected cells were lysed with a Bright-Glo luciferase assay system (Promega, Cat# E2620), and the luminescent signal was measured using a GloMax explorer multimode microplate reader 3500 (Promega). The pseudoviruses were stored at –80°C until use.

Neutralization assay

Neutralization assays were performed as previously described.[1-3,5-8,12,13,15-18] Briefly, the SARS-CoV-2 spike pseudoviruses (counting ~20,000 relative light units) were incubated with serially diluted (120-fold to 87,480-fold dilution at the final concentration) heat-inactivated sera at 37°C for 1 hour. Pseudoviruses without sera were included as controls. Then, an 40 μl mixture of pseudovirus and serum was added to HOS-ACE2/TMPRSS2 cells (10,000 cells/50 μl) in a 96-well white plate. Two days post infection, the infected cells were lysed with a Bright-Glo luciferase assay system (Promega, Cat# E2620), and the luminescent signal was measured using a GloMax explorer multimode microplate reader 3500 (Promega). The assay of each serum sample was performed in triplicate, and the 50% neutralization titer was calculated using Prism 9 (GraphPad Software). The raw data of NT_{50} values are summarized in **Table S4**.

Data availability

Dataset used in the epidemic dynamics analysis in this study is available from the GISAID database (https://www.gisaid.org; EPI_SET_230113qo). The GISAID supplemental tables for EPI_SET_230113qo is available in the GitHub repository (https://github.com/TheSatoLab/XBB.1.5_short).

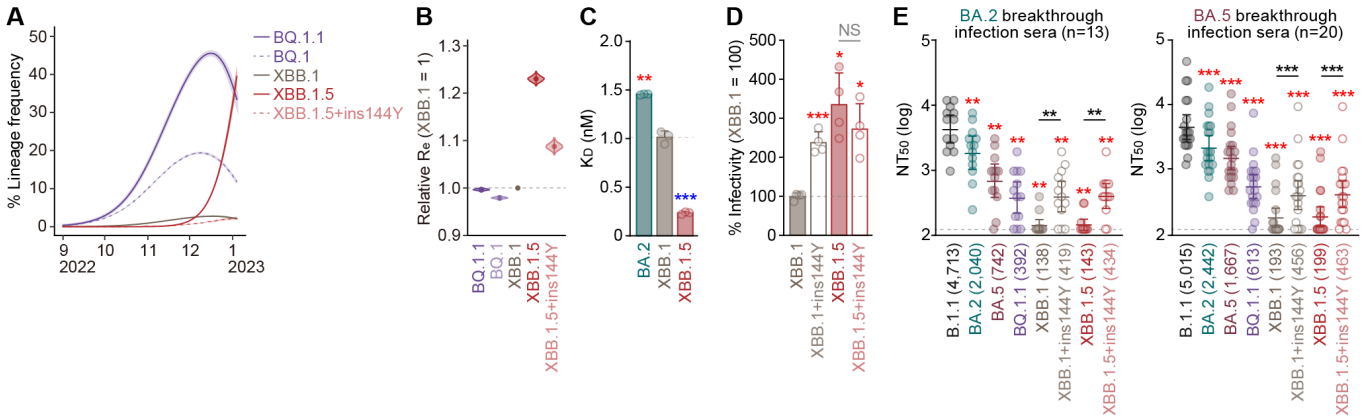

Figure S1. Virological features of Omicron XBB.1.5.

(**A**) Estimated epidemic dynamics of representative viral lineages in the USA (posterior mean, line; 95% Bayesian CI, ribbon).

(**B**) Estimated relative R_e for each viral lineage. The R_e value of XBB.1 is set at 1. The posterior (violin), posterior mean (dot), and 95% CI (line) are shown. The raw data are summarized in **Table S2**.

(**C**) Binding affinity of the RBD of SARS-CoV-2 S protein to the human ACE2 receptor by yeast surface display. The dissociation constant (K_D) value indicating the binding affinity of the RBD of the SARS-CoV-2 S protein to soluble ACE2 when expressed on yeast is shown.

(**D**) Lentivirus-based pseudovirus assay. HOS-ACE2/TMPRSS2 cells were infected with pseudoviruses bearing each S protein. The amount of input virus was normalized based on the amount of HIV-1 p24 capsid protein. The percent infectivity compared to that of the virus pseudotyped with the XBB.1 S protein are shown. NS, no statistical significance.

(**E**) Neutralization assay. Assays were performed with pseudoviruses harboring the S proteins of B.1.1, BA.2, BA.5, BQ.1.1, XBB.1, XBB.1+ins144Y, XBB.1.5, and XBB.1.5+ins144Y. Convalescent sera from fully vaccinated individuals who had been infected with BA.2 after full vaccination (9 2-dose vaccinated and 4 3-dose vaccinated; time interval between the last vaccination and infection, 4–299 days; 11–61 days after testing. n=13 in total; average age: 45 years, range: 24–82 years, 62% male) (left) and those who had been infected with BA.5 after full vaccination (2 2-dose vaccinated, 17 3-dose vaccinated and 1 4-dose vaccinated; time interval between the last vaccination and infection, 66–310 days; 10–23 days after testing. n=20 in total; average age: 51 years, range: 25–73 years, 45% male) (right) were used. The number in parenthesis indicates the average of NT_{50} values. The horizontal dashed line indicates the detection limit (120-fold). In **C** and **D**, assays were performed in triplicate (**C**) or quadruplicate (**D**). The presented data are expressed as the average ± SD. The horizontal dashed line indicates the value of XBB.1. Red and blue asterisks indicate increased and decreased values, respectively. In **E**, each dot indicates the result of an individual replicate. Assays for each serum sample were performed in triplicate to determine the NT_{50}. Each dot represents one NT_{50} value, and the

geometric mean and 95% CI are shown. Red asterisks indicate decreased NT50s. Information on the convalescent donors is summarized in **Table S1**, and the raw data of NT_{50} values are summarized in **Table S4**. Statistically significant differences (*, $P < 0.01$; **, $P < 0.001$; ***, $P < 0.0001$) versus XBB.1 were determined by two-sided Student's *t* tests (**C and D**) or two-sided Wilcoxon signed-rank tests (**E**). In **E**, statistically significant differences (***, $P < 0.0001$) between with or without ins144Y were determined by two-sided Wilcoxon signed-rank tests and indicated with black asterisks.

Table S1. Human sera used in this study

SARS-CoV-2 variant infected	Donor ID	Sex	Age	Date of test (YYYY/MM/DD)	Date of sampling (YYYY/MM/DD)	Infection before vaccination?	Vaccine	Date of 1st vaccination (YYYY/MM/DD)	Date of 2nd vaccination (YYYY/MM/DD)	Date of 3rd vaccination (YYYY/MM/DD)	Date of 4rd vaccination (YYYY/MM/DD)	Time interval between the last vaccination and infection (day)
BA.2	P378	Male	43	2022/03/28	2022/04/10	No	BNT162b2	2021/10/10	2021/10/31			148
BA.2	P398	Male	48	2022/04/13	2022/04/30	No	BNT162b2	2021/09/18	2021/10/09	2022/04/09		4
BA.2	P407	Male	29	2022/05/01	2022/05/12	No	mRNA-1273	2021/09/13	2021/10/11			202
BA.2	P401	Male	35	2022/04/22	2022/05/05	No	BNT162b2	2021/09/09	2021/09/30			204
BA.2	P412	Female	82	2022/05/04	2022/05/26	No	BNT162b2	2021/06/11	2021/07/09			299
BA.2	6449	Male	43	2022/04/03	2022/04/23	No	BNT162b2	2021/08/13	2021/09/11			204
BA.2	6355	Male	50	2022/04/02	2022/04/20	No	Not applicable	2021/04/28	2021/05/19	2022/01/19		73
BA.2	6547	Male	54	2022/04/06	2022/04/22	No	BNT162b2	2021/08/25	2021/09/15			203
BA.2	7951	Female	71	2022/04/25	2022/05/12	No	Mix	2021/06/20 (BNT162b2)	2021/07/16 (BNT162b2)	2022/02/16 (mRNA-1273)		68
BA.2	8645	Female	41	2022/05/07	2022/05/20	No	BNT162b2	2021/05/23	2021/06/13	2022/01/20		107
BA.2	8682	Female	25	2022/05/08	2022/05/24	No	BNT162b2	2021/09/03	2021/09/27			223
BA.2	5949	Male	24	2022/03/22	2022/05/22	No	mRNA-1273	2021/08/05	2021/09/02			201
BA.2	8796	Female	34	2022/05/10	2022/06/05	No	BNT162b2	2021/09/26	2021/10/17			205
BA.5	P427	Female	49	2022/07/06	2022/07/25	No	Not applicable	2021/07/30	2021/08/25	2022/03/18		110
BA.5	P440	Male	25	2022/07/24	2022/08/07	No	BNT162b2	2021/11/24	2021/12/15			221
BA.5	P439	Female	73	2022/07/23	2022/08/08	No	BNT162b2	2021/06/19	2021/07/20	2022/02/04 (mRNA-1273)		169
BA.5	P451	Female	55	2022/07/29	2022/8/12	No	BNT162b2	2021/04/26	2021/05/20	2022/01/18		192
BA.5	P456	Male	44	2022/08/04	2022/08/14	No	BNT162b2	2021/08/11	2021/09/01	2022/03/13 (mRNA-1273)		144
BA.5	P455	Male	29	2022/08/03	2022/08/17	No	mRNA-1273	2021/07/26	2021/08/27	2022/04/18		107
BA.5	P464	Male	63	2022/08/08	2022/08/19	No	BNT162b2	2021/08/08	2021/08/29	2022/04/07 (mRNA-1273)		123
BA.5	9341	Male	56	2022/06/12	2022/06/30	No	BNT162b2	2021/08/10	2021/08/31	2022/03/18		86
BA.5	9584	Male	55	2022/07/08	2022/07/25	No	BNT162b2	2021/07/14	2021/08/05	2022/03/22		108
BA.5	11318	Female	51	2022/07/24	2022/08/05	No	BNT162b2	2021/09/01	2021/09/22	2022/05/19 (mRNA-1273)		66
BA.5	23S-08	Male	25	2022/07/23	2022/08/08	No	BNT162b2	2021/04/27	2021/05/18	2022/01/11		193
BA.5	11597	Female	41	2022/07/26	2022/08/08	No	BNT162b2	2021/04/30	2021/05/21	2022/01/11		196
BA.5	10978	Female	46	2022/07/22	2022/08/11	No	BNT162b2	2021/08/27	2021/09/17	2022/05/15		68
BA.5	10826	Male	63	2022/07/21	2022/08/11	No	BNT162b2	2021/07/27	2021/08/17	2022/03/04	2022/08/09 (mRNA-1273)	139
BA.5	11079	Female	65	2022/07/23	2022/08/11	No	mRNA-1273	2021/07/08	2021/08/05	2022/03/17		128
BA.5	14847	Female	70	2022/08/13	2022/08/25	No	BNT162b2	2021/07/13	2021/08/20	2022/03/08 (mRNA-1273)		158
BA.5	13180	Female	63	2022/08/04	2022/08/25	No	BNT162b2	2021/07/16	2021/08/06	2022/03/08 (mRNA-1273)		149
BA.5	12912	Male	64	2022/08/02	2022/08/25	No	mRNA-1273	2021/09/02	2021/09/30	2022/04/01		123
BA.5	14956	Female	33	2022/08/13	2022/08/28	No	BNT162b2	2021/09/06	2021/10/07			310
BA.5	15707	Female	52	2022/08/16	2022/08/29	No	BNT162b2	2021/08/07	2021/08/28	2022/04/03		135

Table S2. Information on estimated relative Re value for each viral lineage

PANGO lineage	Posterior mean	Posterior 2.5 percentile	Posterior 97.5 percentile	R-hat value	Effective sampling size (ESS_bulk)	Effective sampling size (ess_tail)
XBB.1.5	1.234	1.222	1.246	1.002	1952.4	4951.0
XBB.1.5+ins144Y	1.089	1.075	1.102	1.001	2894.9	7866.7
XBB.2	1.002	0.993	1.011	1.003	1729.2	4963.0
BQ.1.1	0.997	0.992	1.001	1.009	390.3	854.0
CK.1	0.996	0.987	1.005	1.003	1624.0	4448.7
CQ.2	0.991	0.981	1.001	1.002	1762.0	5079.7
BQ.1	0.979	0.975	0.983	1.009	395.6	943.6
BA.5.2.35	0.966	0.958	0.974	1.002	1484.2	4403.4
BA.2.75	0.941	0.936	0.945	1.008	436.2	1056.3
BA.5.1.27	0.939	0.934	0.945	1.004	790.9	2159.1
BA.5.2.6	0.938	0.933	0.943	1.006	577.2	1502.3
BF.14	0.933	0.926	0.940	1.002	1025.7	2773.6
BF.7.4.1	0.933	0.927	0.938	1.004	710.3	2026.7
CM.2	0.930	0.923	0.937	1.003	1191.1	3681.0
BA.5.2.34	0.927	0.921	0.932	1.005	673.0	1735.0
BF.7	0.920	0.916	0.924	1.008	435.9	1043.3
BF.11	0.917	0.912	0.922	1.006	599.0	1661.9
BE.1.1.1	0.916	0.909	0.922	1.003	933.2	2275.5
BA.5.2.23	0.915	0.909	0.921	1.004	838.2	2615.1
BF.7.4	0.915	0.910	0.920	1.006	663.8	1894.7
BA.5.1.18	0.898	0.893	0.904	1.005	714.5	1916.6
BA.5.9	0.893	0.886	0.900	1.003	1134.7	3412.8
BF.13	0.885	0.879	0.891	1.004	831.7	2318.6
BA.5.1.5	0.884	0.879	0.889	1.005	734.6	2080.0
BE.1.1	0.884	0.879	0.888	1.006	537.7	1402.8
BF.26	0.881	0.876	0.885	1.007	509.9	1284.5
BA.5.5.1	0.871	0.866	0.877	1.004	868.0	2493.4
BA.5.2.3	0.869	0.862	0.875	1.002	1198.5	3518.6
BA.5.2.20	0.866	0.861	0.871	1.005	667.4	2045.0
BA.5.1.22	0.865	0.860	0.870	1.005	718.1	2217.6
BA.5.2.31	0.865	0.858	0.871	1.003	1054.5	2983.0
BE.1.4	0.862	0.856	0.869	1.003	1173.4	3736.9
BA.5.2	0.862	0.858	0.866	1.009	393.4	862.8
BA.5.1.10	0.861	0.856	0.866	1.006	650.1	1720.5
BA.5.1.6	0.861	0.855	0.868	1.004	1108.2	2816.6
BA.5	0.861	0.857	0.865	1.007	505.0	1329.1
BA.5.2.21	0.861	0.856	0.865	1.005	595.0	1765.2
BF.10	0.859	0.855	0.863	1.008	461.5	1127.6
BA.5.1.3	0.858	0.851	0.865	1.002	1302.3	3986.9
BF.5	0.857	0.853	0.862	1.007	527.5	1417.6
BA.5.2.9	0.856	0.852	0.860	1.007	494.7	1199.0
BA.4.6.5	0.855	0.850	0.861	1.004	808.8	2293.9

BA.5.1	0.855	0.851	0.859	1.008	415.0	957.0
BA.5.1.23	0.855	0.849	0.860	1.004	786.8	1947.4
BA.4.6	0.854	0.850	0.858	1.008	398.5	887.0
BA.5.1.25	0.851	0.845	0.858	1.003	1203.5	3445.9
BA.5.2.1	0.850	0.847	0.854	1.009	383.5	811.7
BE.1	0.849	0.843	0.854	1.005	745.1	2051.5
BA.5.1.30	0.847	0.841	0.853	1.004	999.1	2768.6
BA.5.1.2	0.847	0.840	0.854	1.003	1193.7	3556.3
BA.5.5	0.844	0.840	0.848	1.007	505.6	1218.6
BA.5.2.22	0.843	0.836	0.850	1.003	1291.3	4064.0
BF.27	0.837	0.831	0.843	1.003	909.9	2698.9
BF.21	0.836	0.829	0.842	1.003	1081.6	3131.9
BA.5.1.1	0.831	0.825	0.836	1.005	846.8	2285.5
BF.8	0.830	0.823	0.837	1.002	1350.1	3848.4
BA.5.6	0.819	0.815	0.824	1.007	577.2	1479.4
BE.3	0.817	0.810	0.823	1.002	1237.1	3884.6
BA.4.1	0.800	0.793	0.806	1.002	1496.2	4352.3

The Re value of XBB.1 is set at 1.

Table S3. Primers used in this study

Primer name	Primer sequence (5'-to-3')	Use
Omicron universal Fw	cactatagggcgaattgggtaccatgtttgtgttcctggt	Preparation of S expression plasmid
BA2 Rv	agctccaccgcggtggcggccgctcaggtgtagtgcagtttca	Preparation of S expression plasmid
pC-S_XBB_S486P_Fwd	aatggagtggccggcCCCaactgttacAGCcca	Preparation of S expression plasmid
pC-S_XBB_S486P_Rev	tggGCTgtaacagttGGGgccggccactccatt	Preparation of S expression plasmid
pC-S_BA.2_F486P_Fwd	aatggagtggccggcCCCaactgttactttcca	Preparation of S expression plasmid
pC-S_BA.2_F486P_Rev	tggaaagtaacagttGGGgccggccactccatt	Preparation of S expression plasmid
pC-S_XBB_insY144_Fwd	ccattcctgGACgtcTACtacCAGaagaacaac	Preparation of S expression plasmid
pC-S_XBB_insY144_Rev	gttgttcttCTGgtaGTAgacGTCcaggaatgg	Preparation of S expression plasmid
XBB_F486P_F	CAGGCCGGTAACAAACCTTGTAATGGTGTTGCAGGTCC AAATTGTTACTCTCCTTTACAATCATATGGTTTCC	Preparation of S RBD expression plasmid

Table S4. Raw data of neutralization assay

SARS-CoV-2 variant infected	Donor ID	B.1.1	BA.2	BA.5	BQ.1.1	XBB.1	XBB.1 +ins144Y	XBB1.5	XBB.1.5 +ins144Y
BA.2	P378	11653	8136	2453	1833	120	2024	120	1938
BA.2	P398	7762	6959	1468	1053	120	1012	120	703.2
BA.2	P407	2041	1049	553.9	574.6	120	745.4	120	705.7
BA.2	P401	10800	3573	3456	941.5	360.2	1295	283.1	650.6
BA.2	P412	14109	2707	925.6	201	250.5	426.9	165.5	433.8
BA.2	6449	7909	3297	1054	201.3	120	235.6	305.5	270.5
BA.2	6355	3449	2200	945.8	958.1	120	613.7	120	435.8
BA.2	6547	3143	1210	362.6	120	120	120	120	707.6
BA.2	7951	1109	280.7	134.4	120	120	120	120	120
BA.2	8645	6932	3175	1002	467.9	120	551.8	134.6	409.8
BA.2	8682	2497	1530	511	366.5	120	305	120	364
BA.2	5949	5851	2424	839.5	437.2	120	342.8	130.8	393.6
BA.2	8796	2092	635.2	155.5	120	120	120	120	120
P value (vs B.1.1)		-	0.0002	0.0002	0.0002	0.0002	0.0002	0.0002	0.0002
P value (vs BA.2)		-	-	0.0002	0.0002	0.0002	0.0002	0.0002	0.0002
P value (vs BA.5)		-	-	-	0.0049	0.0005	0.0039	0.0005	0.0103
P value (vs with ins144Y)						0.002	-	0.002	-
BA.5	P427	5125	3944	2351	1292	132.6	1164	197.3	600.9
BA.5	P440	1291	440.3	514.3	120	120	120	120	120
BA.5	P439	45195	22133	16231	8750	1152	9792	1649	10049
BA.5	P451	24313	10225	10311	2027	1513	3112	2099	2923
BA.5	P456	4414	3690	2381	740.3	120	123.2	120	166.4
BA.5	P455	2273	1010	685.7	380	120	120	120	158.6
BA.5	P464	3998	2051	2110	442.8	120	172.2	120	394.9
BA.5	9341	25761	7569	4057	1059	274.8	336.1	231	631.2
BA.5	9584	3273	887.2	763.9	351.6	120	120	120	120
BA.5	11318	3370	1691	1908	342.7	120	139.5	120	144.4
BA.5	23S-08	3187	4656	2201	714	563.2	583.8	491.5	650.3
BA.5	11597	2434	1727	1096	161.5	164.1	259.1	133.9	229.3
BA.5	10978	2331	1300	956.8	526.8	120	753.3	120	421.9
BA.5	10826	4450	1290	987	778.9	120	1128	120	953.8
BA.5	11079	5767	2101	1187	331.9	176.1	560.4	216	610.9
BA.5	14847	11752	5373	1528	250.4	120	644.7	120	813.3
BA.5	13180	3112	1791	459.1	611.7	120	436.5	120	266.7
BA.5	12912	13863	4734	4497	1076	546.4	874.3	453.2	1008
BA.5	14956	2977	1353	889.2	1117	120	378.2	120	353.3
BA.5	15707	1746	957.6	880.9	450.9	120	366.1	120	294.6
P value (vs B.1.1)		-	< 0.0001	< 0.0001	< 0.0001	< 0.0001	< 0.0001	< 0.0001	< 0.0001
P value (vs BA.2)		-	-	0.0007	< 0.0001	< 0.0001	< 0.0001	< 0.0001	< 0.0001
P value (vs BA.5)		-	-	-	< 0.0001	< 0.0001	< 0.0001	< 0.0001	< 0.0001
P value (vs with ins144Y)						0.0001	-	0.0001	-

Consortia

The Genotype to Phenotype Japan (G2P-Japan) Consortium

The Institute of Medical Science, The University of Tokyo, Japan
Izumi Kimura, Naoko Misawa, Arnon Plianchaisuk, Daniel Sauter, Lin Pan, Mai Suganami, Adam Strange, Naomi Ohsumi, Mika Chiba, Ryo Yoshimura, Kyoko Yasuda, Keiko Iida

Hokkaido University, Japan
Takasuke Fukuhara, Tomokazu Tamura, Rigel Suzuki, Saori Suzuki, Hayato Ito, Keita Matsuno, Hirofumi Sawa, Naganori Nao, Shinya Tanaka, Masumi Tsuda, Lei Wang, Yoshikata Oda, Marie Kato, Zannatul Ferdous, Hiromi Mouri, Kenji Shishido

Tokyo Metropolitan Institute of Public Health, Japan
Kenji Sadamasu, Kazuhisa Yoshimura, Hiroyuki Asakura, Isao Yoshida, Mami Nagashima

Tokai University, Japan
So Nakagawa, Jiaqi Wu

Kyoto University, Japan
Kotaro Shirakawa, Akifumi Takaori-Kondo, Kayoko Nagata, Yasuhiro Kazuma, Ryosuke Nomura, Yoshihito Horisawa, Yusuke Tashiro, Yugo Kawai, Kazuo Takayama, Rina Hashimoto, Sayaka Deguchi, Yukio Watanabe, Ayaka Sakamoto, Naoko Yasuhara, Takao Hashiguchi, Tateki Suzuki, Kanako Kimura, Jiei Sasaki, Yukari Nakajima, Hisano Yajima

Hiroshima University, Japan
Takashi Irie, Ryoko Kawabata

Kyushu University, Japan
Kaori Tabata

Kumamoto University, Japan
Terumasa Ikeda, Hesham Nasser, Ryo Shimizu, MST Monira Begum, Otowa Takahashi, Kimiko Ichihara, Takamasa Ueno, Chihiro Motozono, Mako Toyoda

University of Miyazaki, Japan
Akatsuki Saito, Maya Shofa, Yuki Shibatani, Tomoko Nishiuchi

Acknowledgments

We would like to thank all members of The Genotype to Phenotype Japan (G2P-Japan) Consortium. We thank Dr. Kenzo Tokunaga (National Institute of Infectious Diseases, Japan) for sharing materials and Dr. Jin Kuramochi (Interpark Kuramochi Clinic, Japan) for sharing human sera. We gratefully acknowledge the numerous laboratories worldwide that have provided sequence data and metadata to GISAID. A full list of originating and submitting laboratories for the sequences used in our analysis can be found at https://www.gisaid.org using the EPI-SET-ID: EPI_SET_230113qo.

Supplementary References

1. Yamasoba D, Kimura I, Nasser H, et al. Virological characteristics of the SARS-CoV-2 Omicron BA.2 spike. *Cell* 2022.
2. Kimura I, Yamasoba D, Tamura T, et al. Virological characteristics of the novel SARS-CoV-2 Omicron variants including BA.4 and BA.5. *Cell* 2022; **185**(21): 3992-4007 e16.
3. Saito A, Tamura T, Zahradnik J, et al. Virological characteristics of the SARS-CoV-2 Omicron BA.2.75 variant. *Cell Host Microbe* 2022.
4. Motozono C, Toyoda M, Zahradnik J, et al. SARS-CoV-2 spike L452R variant evades cellular immunity and increases infectivity. *Cell Host Microbe* 2021; **29**(7): 1124-36.
5. Uriu K, Kimura I, Shirakawa K, et al. Neutralization of the SARS-CoV-2 Mu variant by convalescent and vaccine serum. *N Engl J Med* 2021; **385**(25): 2397-9.
6. Yamasoba D, Kosugi Y, Kimura I, et al. Neutralisation sensitivity of SARS-CoV-2 omicron subvariants to therapeutic monoclonal antibodies. *Lancet Infect Dis* 2022; **22**(7): 942-3.
7. Ito J, Suzuki R, Uriu K, et al. Convergent evolution of the SARS-CoV-2 Omicron subvariants leading to the emergence of BQ.1.1 variant. *BioRxiv* 2022: doi: https://doi.org/10.1101/2022.12.05.519085.
8. Tamura T, Ito J, Uriu K, et al. Virological characteristics of the SARS-CoV-2 XBB variant derived from recombination of two Omicron subvariants. *BioRxiv* 2022: doi: https://doi.org/10.1101/2022.12.27.521986.
9. Niwa H, Yamamura K, Miyazaki J. Efficient selection for high-expression transfectants with a novel eukaryotic vector. *Gene* 1991; **108**(2): 193-9.
10. Zahradnik J, Dey D, Marciano S, et al. A protein-engineered, enhanced yeast display platform for rapid evolution of challenging targets. *ACS Synth Biol* 2021; **10**(12): 3445-60.
11. Zahradnik J, Marciano S, Shemesh M, et al. SARS-CoV-2 variant prediction and antiviral drug design are enabled by RBD in vitro evolution. *Nat Microbiol* 2021; **6**(9): 1188-98.
12. Kimura I, Kosugi Y, Wu J, et al. The SARS-CoV-2 Lambda variant exhibits enhanced infectivity and immune resistance. *Cell Rep* 2022; **38**(2): 110218.
13. Ferreira I, Kemp SA, Datir R, et al. SARS-CoV-2 B.1.617 mutations L452R and E484Q are not synergistic for antibody evasion. *J Infect Dis* 2021; **224**(6): 989-94.
14. Ozono S, Zhang Y, Ode H, et al. SARS-CoV-2 D614G spike mutation increases entry efficiency with enhanced ACE2-binding affinity. *Nat Commun* 2021; **12**(1): 848.
15. Fujita S, Kosugi Y, Kimura I, Yamasoba D, The Genotype to Phenotype Japan (G2P-Japan) Consortium, Sato K. Structural Insight into the Resistance of the SARS-CoV-2 Omicron BA.4 and BA.5 Variants to Cilgavimab. *Viruses* 2022; **14**(12): 2677.

16. Uriu K, Cardenas P, Munoz E, et al. Characterization of the immune resistance of SARS-CoV-2 Mu variant and the robust immunity induced by Mu infection. *J Infect Dis* 2022.
17. Saito A, Irie T, Suzuki R, et al. Enhanced fusogenicity and pathogenicity of SARS-CoV-2 Delta P681R mutation. *Nature* 2022; **602**(7896): 300-6.
18. Kimura I, Yamasoba D, Nasser H, et al. The SARS-CoV-2 spike S375F mutation characterizes the Omicron BA.1 variant. *iScience* 2022; **25**(12): 105720.
19. Ozono S, Zhang Y, Tobiume M, Kishigami S, Tokunaga K. Super-rapid quantitation of the production of HIV-1 harboring a luminescent peptide tag. *J Biol Chem* 2020; **295**(37): 13023-30.